Epitaxial Phase Transition of Polystyrene-*b*-Polyisoprene from Hexagonally Perforated Layer to Gyroid Phase in Thin Film

Insun Park, Byeongdu Lee, Jinsook Ryu, Kyuhyun Im, Jinhwan Yoon, Moonhor Ree,* and Taihyun Chang*

Department of Chemistry and Polymer Research Institute, Pohang University of Science and Technology, Pohang 790-784, Korea

Received June 1, 2005; Revised Manuscript Received October 8, 2005

ABSTRACT: We investigated the phase transition behavior from the hexagonally perforated layer (HPL) to the gyroid (G) phase in supported thin film of a polystyrene-*b*-polyisoprene (PS-*b*-PI) diblock copolymer (M_n = 34.0 kg/mol, wt_{PI} = 0.634) by grazing-incidence small-angle X-ray scattering. After annealing at 120 °C, the PS-*b*-PI thin film spin-coated on silicon wafer exhibited HPL morphology with its lamellae highly oriented parallel to the substrate up to a thickness as much as 1 μm. The interface-induced orientation allowed us to obtain a well-developed diffraction pattern in the absence of external mechanical strain to align the domains. The comparison with the computer-simulated diffraction pattern revealed that the HPL structure has mosaic grains oriented randomly in-plane with ABC stacking and undetectable amount of AB stacking. Upon heating, the HPL phase undergoes a phase transition to the G phase. The phase transition occurred epitaxially converting the HPL layers to the {121} planes of the G structure maintaining the G {121} plane oriented parallel to the substrate. This behavior is in contrast with the HPL to G phase transition found from the shear-oriented HPL samples, in which the G {121} plane is randomly oriented around the G [111] axis.

Introduction

The hexagonally perforated layer (HPL) structure is found in block copolymers over a narrow composition range.[1−3] The HPL morphology is also known to be metastable and appears at a limited temperature window between the stable lamella and gyroid morphologies. Despite the limited accessibility, the HPL phase has drawn much attention due to its intriguing structural characteristics. For example, the stacking sequence of the perforation in HPL morphology has been one of the subjects of interest. The stacking sequences may be modeled as ABC and AB arrangements. The ABC stacking has a rhombohedral (trigonal) symmetry (space group $R\bar{3}m$) whereas the AB stacking has a hexagonal symmetry (space group $P6_3/mmc$). In the special case of close-packed structures, the ABC and AB stacking structures correspond to face-centered cubic and hexagonally close-packed phases, respectively. The free energy calculations for the two HPL structures showed that the two states are metastable in the intermediate segregation limit with nearly degenerate free energy.[2,4]

The preferred stacking structure cannot be determined without regular order. Alignment of the layer structure by shear allowed the study of the perforation arrangement. Ahn et al. reported that the shear-induced HPL phase in a PS-*b*-PI diblock copolymer has a trigonal ABC stacking sequence from the analysis of the SAXS pattern along the shear direction.[5] More recently, Zhu et al. showed from the TEM and SAXS study on a highly shear-aligned HPL structure of a PS-*b*-PEO block copolymer that the HPL phase contains a mixed structure of trigonal twins (ABC and ACB) as the major components and minor hexagonal (AB) structure.[6,7] They also reported that the plastic deformation under a mechanical shear induced various dislocations to yield the mixed structure.

Such oriented HPL structure is known to undergo epitaxial phase transition to gyroid (G) phase upon heating.[2,3,5,7−9] The G phase obtained from the shear-oriented HPL (the lamellae aligned perpendicular to the shear plane (*xz* plane) and the incident beam is parallel to the gradient axis (*y* axis); see Figure 4) shows a 10-spot scattering pattern of {121} reflections.[2,3,9] The same scattering pattern was also observed from the G phase grown from the shear-oriented cylinder phase in concentrated block copolymer solution.[10] The 10-spot scattering pattern characteristic of the G phase indicates that the G phase is constituted of a directionally oriented polycrystal, in which the [111] axis lies along the shear direction while the {121} and {220} planes are randomly oriented around this axis. The epitaxial transition is known to convert the HPL layer ({003} plane in hexagonal lattice indexing) to the G {121} plane.[8,10] A perfect epitaxial transition of a HPL single crystal would yield only six first-order {121} reflections in the scattering geometry described above.[2] The origin of such an orientational defect developed in the G phase for the shear-aligned samples is not elucidated completely but tentatively attributed to the distortion during the morphological transformation.[2,9]

Another way to orient the microphase-separated block copolymer in the absence of mechanical shear is to confine the system into a restricted geometry such as a thin film. In block copolymer films on substrate, the differences in affinity of the block components at the interface control the orientation of lamellae or cylinders.[11−13] The orientation is a result of interfacial energy minimization between air/polymer and polymer/substrate. The morphology in block copolymer thin films has recently been a subject of increasing interest due

* Corresponding authors. Taihyun Chang: Tel +82-54-279-2109; Fax +82-54-279-3399; e-mail tc@postech.edu. Moonhor Ree: Tel +82-54-279-2120; Fax +82-54-279-3399; e-mail ree@postech.edu.

10.1021/ma051137i CCC: $30.25
Published on Web 11/12/2005

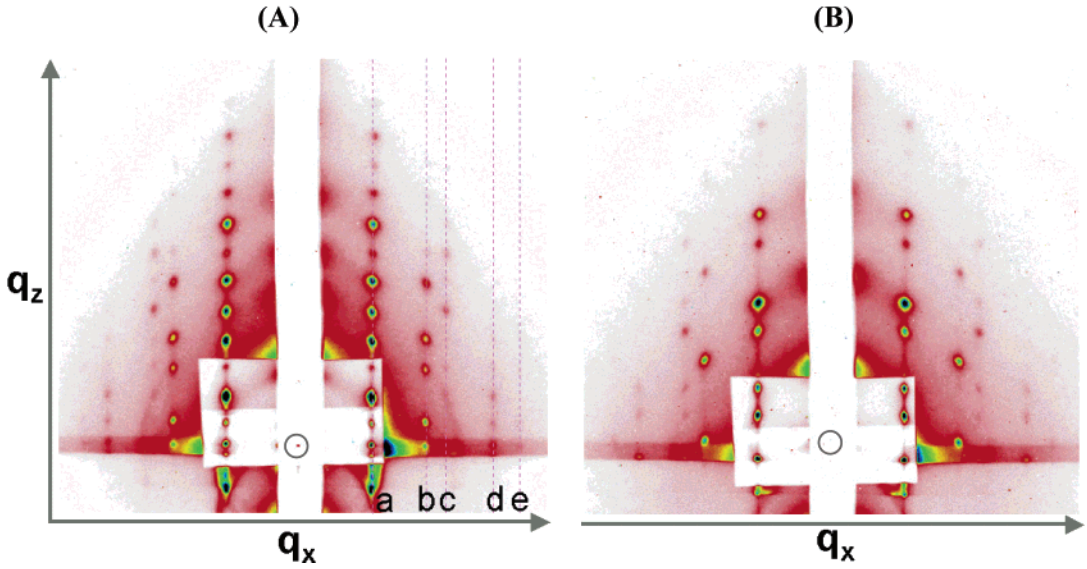

Figure 1. GISAXS profiles of PS-*b*-PI thin film spin-coated on silicon wafer (thickness: 1.25 μm) at different incident angles of (A) 0.22° and (B) 0.24°. The films were annealed at 120 °C in vacuo for 1 day.

to the potential applications such as surface patterning, lithography, templates for the fabrication of information storage devices, magnetic and optical materials, nanowires, and ultrathin membranes.[14,15] However, the phase behavior such as order−order transition or order−disorder transition in thin film has not been established well until now even though a variety of deviations from the bulk structures have been observed.[15,16]

In this study, the transition from HPL to G structures of a PS-*b*-PI diblock copolymer in the thin film state was investigated by grazing-incidence SAXS (GISAXS).[17−19] By virtue of the interface-induced orientation, we could obtain a diffraction pattern to a very high order without applying any mechanical strain to align the domains. The perforations in the HPL phase were found to have a nearly pure ABC stacking structure and a near perfect epitaxial transition of the HPL {003} layer to the G {121} plane was observed.

Experimental Section

Characterization of Diblock Copolymer. PS-*b*-PI diblock copolymer was synthesized by anionic polymerization[20,21] and characterized with SEC. Two SEC mixed bed columns (Polymer Lab., PL mixed C × 2) were used, and the eluent was THF (HPLC grade). Chromatograms were recorded with a multiangle laser light scattering detector (Wyatt, mini-DAWN) and a refractive index detector (Wyatt, Opti-Lab). The composition of the block copolymers was determined by ^{1}H NMR spectroscopy (Bruker, DPX-300). The number-average molecular weight of the PS-*b*-PI and the weight fraction of the PI block are 34.0 kg/mol and 0.634, respectively.

Preparation of Thin Film. Silicon wafers were cleaned with piranha solution (concentrated H_2SO_4/30% H_2O_2 = 3/1 (v/v)) for 1 h. The substrate was thoroughly rinsed with deionized water. PS-*b*-PI diblock copolymer was dissolved in toluene (HPLC grade) at 10 wt % and spin-coated onto a silicon wafer at 2000 rpm. The polymer film was vacuum-dried at room temperature for 12 h to evaporate the residual solvent completely and annealed at 120, 140, and 160 °C for 1 day in vacuo.

GISAXS Measurements. GISAXS measurements are carried out at the 4C1 and 4C2 beamline at the Pohang Accelerator Laboratory, Pohang, Korea.[22] The wavelength of X-rays from the bending magnet was monochromatized to the wavelength of 1.54 Å. A CCD (Princeton Instruments) detector was used, and the sample-to-detector distance was 2.3 m. The critical angle of the polymer film and the silicon wafer was calculated from the electron density as 0.15° and 0.22°, respectively. The samples were mounted on a *z*-axis goniometer placed in a vacuum chamber. The incident angle was set to 0.22−0.24°, and the typical collection time of the scattering intensity was 100−600 s.

Results and Discussion

In bulk, the PS-*b*-PI diblock copolymer showed HPL morphology after annealing at 120 °C for 1 day. Upon heating at a rate of 2 °C/min, its morphology changes to G phase at 170 °C and to disordered phase at 230 °C as reported previously.[23] The order-to-order transition is slow, and a substantial overheating was involved for the phase transition since the same sample shows the G phase after annealing at 130 °C for 1 day. It would not be something specific for this sample since the similar level of overheating due to different heating rates can be found in the literature.[24] The phase transition slows down even more in thin film. Therefore, the real-time GISAXS measurements take impractically long time to observe the phase transition, and in this study, individual thin film samples were prepared and annealed at different temperatures for 1 day.

Figure 1A shows the GISAXS pattern of the PS-*b*-PI annealed at 120 °C for 1 day. The film thickness measured by ellipsometry was 1254 ± 4 nm. The X-ray beam impinges on the polymer film at an incident angle of 0.22°. The vertical strip in the middle is the shadow of the beam stop to block the X-ray beam reflected directly from the Si wafer surface which is very intense near the critical angle. Also, the strong scattering peaks at the low q region were partially blocked with a thin beam stop to enhance the visibility of the peaks at higher q. Several vertical arrays of the scattering peaks show up, and the clear appearance of the higher order Bragg's spots indicates the highly regular stacks in both in-plane and out-of-plane directions. This scattering pattern is consistent with the hexagonally perforated layer structure as elaborated below.

The relative positions of the vertical peak arrays, a−e, are $1{:}\sqrt{3}{:}\sqrt{4}{:}\sqrt{7}{:}\sqrt{9}$, corresponding to the in-plane hexagonal arrangement of the microdomains but randomly oriented. The interpretation along the out-of-plane (z) direction is more complicated due to the

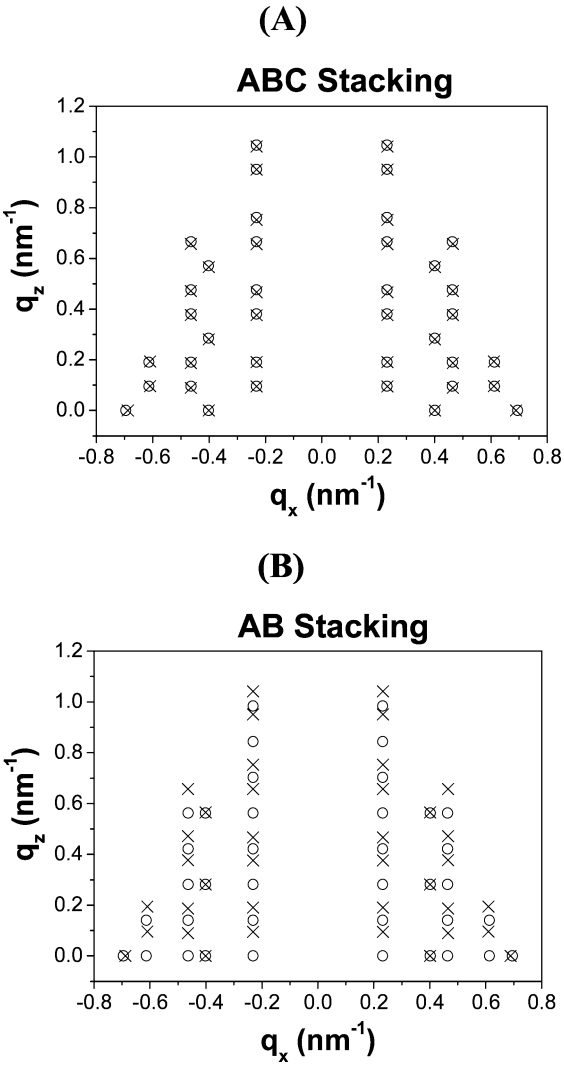

Figure 2. Comparison of the identifiable GISAXS peak positions (×) and the simulated results (○) of the HPL structure having (A) ABC stacking (hexagonal lattice of a_h = 31.3 nm and c_h = 66.1 nm equivalent to the rhombohedral lattice of a_R = 28.5 nm and α = 66.6°) and (B) AB stacking (hexagonal lattice of a_h = 31.3 nm and c_h = 44.0 nm).

overlapped scattering peaks originating from both incident and reflected X-ray beams. They can be sorted out by changing the incident angle.[18] The GISAXS pattern measured at an incident angle of 0.24° is displayed in Figure 1B. The scattering intensity, in particular at high scattering angles, from the reflected beam decreases sharply due to the low reflectivity at the high incident angle (far from the critical angle) and the relative scattering peak positions from the incident and reflected beam change. Matching the positions of the directly reflected beam (marked by ○) in Figure 1A,B, the peaks appearing at the invariable positions are the scattering peaks originating from the X-ray beam reflected from the Si wafer surface.

Another effect we need to consider is the refraction at the air−polymer interface. The refraction shifts the scattering peak position to slightly higher angles along the out-of-plane direction, which is more serious at low q.[18] After the necessary correction considering these effects, the identifiable scattering peaks are displayed in Figure 2. In Figure 2A,B, the diffraction pattern (×) is compared with the computer simulated pattern (○) for an ABC stacking structure with the best fit lattice parameters (rhombohedral lattice, a_R = 28.5 nm and α = 66.6°; in hexagonal lattice, a_h = 31.3 nm and c_h = 66.1 nm) and an AB stacking with a layer spacing and a perforation distance equivalent to the ABC stacking (hexagonal lattice, a_h = 31.3 nm and c_h = 44.0 nm). The hexagonal lattice indexing will be used for the HPL structure in this paper. In the simulation, the perforated layer grains are assumed to be randomly oriented in plane while the layers are oriented parallel to the substrate surface. The perfect match of the experimental and simulated scattering pattern unambiguously confirms that the block copolymer thin film has the HPL morphology with ABC type stacking with few stacking faults although we could not exclude the possibility of the existence of a small amount of AB stacking undetectable in the GISAXS patterns.

Ahn et al. concluded from the SAXS pattern of a shear-oriented PS-*b*-PI that the HPL structure has the ABC stacking.[5] Zhu et al. were able to distinguish the ABC and ACB twins by using shear-oriented PS-*b*-PEO samples and reported that the plastic deformation under mechanical shear induced successive stacking faults for HPL phase to have a mixture of majority trigonal twins (ABC and ACB) and minority hexagonal (AB) stacking.[6,7] The scattering patterns shown in Figure 1 evidence the near perfect out-of-plane orientation of the HPL layers while the in-plane orientation of the perforations is absent. In this system, the ABC and ACB stacking are not distinguishable since they would show the identical scattering pattern when rotated by 60° normal to the layer plane while no trace of AB stacking was detected. Therefore, we can conclude that the HPL phase of PS-*b*-PI block copolymer thin film on the Si wafer with top oxide layer adopts the ABC stacking sequence with few stacking faults compared with shear-oriented samples.

Figure 3 displays the GISAXS patterns obtained for the PS-*b*-PI thin film annealed at different temperatures for 1 day: (A) 120, (B) 140, and (C) 160 °C. The film annealed at 140 °C shows the appearance of the new scattering peaks from the G structure while the majority of the scattering peaks are still from the HPL structure. In the film annealed at 160 °C for 1 day exhibits a fully developed scattering pattern from the G structure. The semicircular arrangement of the scattering peaks are from the {121} and {220} reflections of the gyroid structure, indicating that the {121} plane, the plane epitaxially grown from the HPL {003} plane, is oriented parallel to the substrate surface. The scattering spots appearing near the equator are diffracted from the incident X-ray beam. Any spot appearing below is likely due to a portion of the incident beam passing over most of the sample and hitting the film just above the trailing edge of the substrate. The detailed interpretation of the GISAXS pattern was reported earlier.[18] The spacing of the HPL {003} plane is 22.0 nm while that of G {121} plane is 24.2 nm. The slow HPL → G phase transition of the PS-*b*-PI sample is likely in part due to the domain spacing mismatch since the closer the d spacings are each other, the easier the phase transformation is expected.[8] In the ∼1 μm thick film, more than 50 HPL layers exist. As the film thickness is reduced, the gyroid phase must become unstable as it cannot exist in the two-dimensional limit.[15] Investigating the thickness effect would be interesting for future experiments.

Such an epitaxially ordered G structure has not been found from the shear-oriented block copolymers while

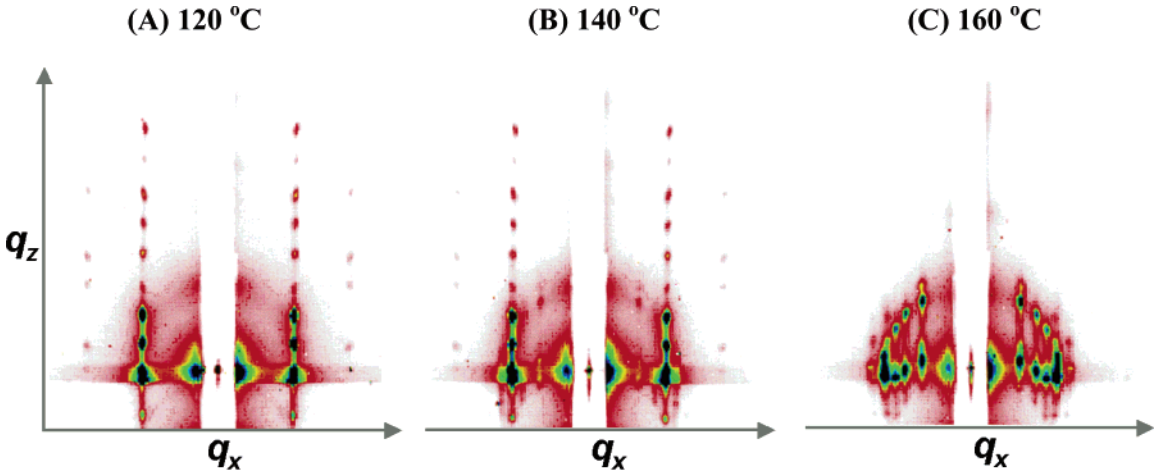

Figure 3. GISAXS profiles (incident angle: 0.22°) of PS-*b*-PI thin films on Si wafer (thickness: 1.25 μm) annealed at different temperatures for 1 day: (A) HPL phase, (B) mostly HPL phase containing a small fraction of G phase, (C) G phase. The spots appearing near the equator in (C) are diffracted from the incident X-ray beam.

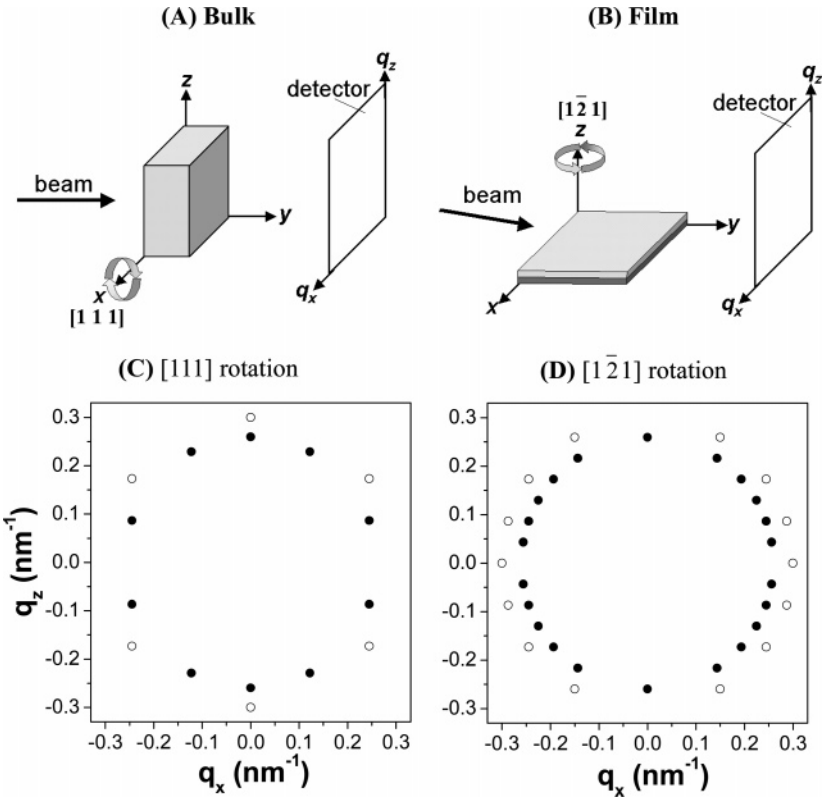

Figure 4. Diffraction geometry and orientation of the G phase in shear-oriented bulk sample (A) and in thin film (B) and the corresponding GISAXS patterns of shear-aligned bulk (C) and thin film (D). Initially HPL layers are oriented parallel to the *xy* plane in both shear-oriented bulk and thin film. Upon thermal annealing, the HPL phase transforms to the G phase in which the HPL layer plane is epitaxially transformed to the G {121} plane in thin film while the G {121} plane of the transformed G phase is randomly oriented around the shear direction, *x* in shear-aligned bulk (●, Bragg reflection spots from {121} planes; ○, Bragg reflection spots from {220} planes). In (A), *x* is the shear direction, *y* is the gradient axis, and *xz* is the shear plane.

the similarly oriented bicontinuous cubic structure was reported in thin films of mesostructured silica recently.[25] While the shear-oriented HPL phase shows a well-aligned, close to a single-crystal-like morphology, the thermally transformed G structure loses the orientational order of the lamellar plane to eventually develop the polygrains whose {121} plane is more or less randomly ordered around the [111] axis, i.e., shear direction. Figure 4 schematically shows the difference between the shear-aligned bulk and the thin film. Figure 4A,C displays the diffraction geometry of the shear-oriented bulk sample and the expected diffraction pattern. The unit cells are randomly oriented around the [111] direction, i.e., the shear axis. The 10-spot pattern from {121} planes and 6-spot pattern from {220} planes appearing at relative q of $\sqrt{6}$ and $\sqrt{8}$ are expected for the geometry and proven experimentally.[2,3,10] On the other hand, Figure 4B,D shows the geometry of the supported thin film and the expected diffraction pattern. It is assumed that the unit cells are oriented randomly around the [1$\bar{2}$1] direction normal to the substrate. The 22-spot scattering pattern from the {121} plane and the 14 spots from the {220} reflection can be observed from the geometry.

It is interesting to note that HPL phases show the same layer alignment in both the bulk and thin film, but after transformation show a substantially different G phase alignment. It means that the HPL {003} plane is epitaxially transformed to the G {121} plane in the supported film while such an epitaxial relationship is partially broken during the phase transition in bulk. In the thin film, the distortion during the transition does not occur, and the transition follows the perfect epitaxial relationship between the layer planes in the two phases. It is likely to reflect the strong substrate effect keeping the rotation or tilt of the lamellae from the substrate surface, which is absent in the shear-oriented bulk system. In the sheared bulk, some degree of imperfection in the microdomain orientation exists even in the best circumstances such as found by Zhu et al.,[7] which may induce the distortion during the phase transition to the highly symmetric bicontinuous cubic phase.[2,9] In addition, it may be also due to the difference in the morphological purity of the HPL phase between bulk and thin film. The HPL phase in bulk is known to exist as a mixture of ABC and AB stacking while such a lattice distortion is largely absent in supported thin films. The lack of imperfections in the thin film phase may also account for a part of "overheating" required to initiate the HPL/gyroid transformation.

In summary, the HPL to G phase transition of a PS-*b*-PI thin film spin-coated on silicon wafer was investigated by the GISAXS technique. The layers in HPL structure are well aligned parallel to the film plane without any mechanical shear while the mosaic grains are randomly oriented in plane. The HPL structure shows the ABC stacking, and no detectable amount of the AB stacking was found. The HPL phase undergoes the phase transition to G phase upon heating. The transition in thin film is slower than in bulk and occurs at higher temperature. The HPL to G phase transition occurs in a perfect epitaxial manner between the HPL {003} plane and the G {121} plane.

Acknowledgment. This study was supported in part by KOSEF (Center for Integrated Molecular Systems) and the BK21 program. The GISAXS measurements at PAL were supported by the Ministry of Science and Technology and the POSCO.

References and Notes

(1) Hamley, I. W.; Koppi, K. A.; Rosedale, J. H.; Bates, F. S.; Almdal, K.; Mortensen, K. *Macromolecules* **1993**, *26*, 5959.
(2) Foerster, S.; Khandpur, A. K.; Zhao, J.; Bates, F. S.; Hamley, I. W.; Ryan, A. J.; Bras, W. *Macromolecules* **1994**, *27*, 6922.
(3) Vigild, M. E.; Almdal, K.; Mortensen, K.; Hamley, I. W.; Fairclough, J. P. A.; Ryan, A. J. *Macromolecules* **1998**, *31*, 5702.
(4) Matsen, M. W.; Bates, F. S. *J. Chem. Phys.* **1997**, *106*, 2436.
(5) Ahn, J.-H.; Zin, W.-C. *Macromolecules* **2000**, *33*, 641.
(6) Zhu, L.; Huang, P.; Cheng, S. Z. D.; Ge, Q.; Quirk, R. P.; Thomas, E. L.; Lotz, B.; Wittmann, J.-C.; Hsiao, B. S.; Yeh, F.; Liu, L. *Phys. Rev. Lett.* **2001**, *86*, 6030.
(7) Zhu, L.; Huang, P.; Chen, W. Y.; Weng, X.; Cheng, S. Z. D.; Ge, Q.; Quirk, R. P.; Senador, T.; Shaw, M. T.; Thomas, E. L.; Lotz, B.; Hsiao, B. S.; Yeh, F.; Liu, L. *Macromolecules* **2003**, *36*, 3180.
(8) Hajduk, D. A.; Ho, R.-M.; Hillmyer, M. A.; Bates, F. S.; Almdal, K. *J. Phys. Chem. B* **1998**, *102*, 1356.
(9) Zhao, J.; Majumdar, B.; Schulz, M. F.; Bates, F. S.; Almdal, K.; Mortensen, K.; Hajduk, D. A.; Gruner, S. M. *Macromolecules* **1996**, *29*, 1204.
(10) Wang, C.-Y.; Lodge, T. P. *Macromol. Rapid Commun.* **2002**, *23*, 49.
(11) Henkee, C. S.; Thomas, E. L.; Fetters, L. J. *J. Mater. Sci.* **1988**, *23*, 1685.
(12) Russell, T. P.; Coulon, G.; Deline, V. R.; Miller, D. C. *Macromolecules* **1989**, *22*, 4600.
(13) Anastasiadis, S. H.; Russell, T. P.; Satija, S. K.; Majkrzak, C. F. *J. Chem. Phys.* **1990**, *92*, 5677.
(14) Lazzari, M.; Lopez-Quintela, M. A. *Adv. Mater.* **2003**, *15*, 1583.
(15) Hamley, I. W. *Nanotechnology* **2003**, *14*, R39.
(16) Green, P. F.; Limary, R. *Adv. Colloid Interface Sci.* **2001**, *94*, 53.
(17) Lee, B.; Yoon, J.; Oh, W.; Hwang, Y.; Heo, K.; Jin, K. S.; Kim, J.; Kim, K.-W.; Ree, M. *Macromolecules* **2005**, *38*, 3395.
(18) Lee, B.; Park, I.; Park, S.; Yoon, J.; Kim, J.; Kim, K.-W.; Chang, T.; Ree, M. *Macromolecules* **2005**, *38*, 4311.
(19) Lee, B.; Park, Y.-H.; Hwang, Y.-T.; Oh, W.; Yoon, J.; Ree, M. *Nat. Mater.* **2005**, *4*, 147.
(20) Kwon, K.; Lee, W.; Cho, D.; Chang, T. *Korea Polym. J.* **1999**, *7*, 321.
(21) Lee, W.; Cho, D.; Chang, T.; Hanley, K. J.; Lodge, T. P. *Macromolecules* **2001**, *34*, 2353.
(22) Bolze, J.; Kim, J.; Huang, J.-Y.; Rah, S.; Youn, H. S.; Lee, B.; Shin, T. J.; Ree, M. *Macromol. Res.* **2002**, *10*, 2.
(23) Park, S.; Kwon, K.; Cho, D.; Lee, B.; Ree, M.; Chang, T. *Macromolecules* **2003**, *36*, 4662.
(24) Floudas, G.; Vazaiou, B.; Schipper, F.; Ulrich, R.; Wiesner, U.; Iatrou, H.; Hadjichristidis, N. *Macromolecules* **2001**, *34*, 2947.
(25) Hayward, R. C.; Alberius, P. C. A.; Kramer, E. J.; Chmelka, B. F. *Langmuir* **2004**, *20*, 5998.

MA051137I